arXiv:1503.02033v1 [cond-mat.supr-con] 6 Mar 2015

Suppression of charge order by pressure in the cuprate superconductor $YBa_2Cu_3O_y$: Restoring the full superconducting dome

O. Cyr-Choinière,[1] D. LeBoeuf,[1,*] S. Badoux,[1] S. Dufour-Beauséjour,[1] D. A. Bonn,[2,3]
W. N. Hardy,[2,3] R. Liang,[2,3] N. Doiron-Leyraud,[1] and Louis Taillefer[1,3,†]

[1]*Département de physique & RQMP, Université de Sherbrooke, Sherbrooke, Québec J1K 2R1, Canada*
[2]*Department of Physics and Astronomy, University of British Columbia, Vancouver, British Columbia V6T 1Z4, Canada*
[3]*Canadian Institute for Advanced Research, Toronto, Ontario M5G 1Z8, Canada*

(Dated: March 9, 2015)

It has recently become clear that cuprate superconductors have a universal tendency to form charge-density-wave order. A fundamental question is the relation between this charge order and the pseudogap phase. A key feature is that this tendency is strongest at a doping $p \simeq 0.12$, irrespective of the modulation period. Here we show that pressure suppresses charge order in $YBa_2Cu_3O_y$, but does not affect the pseudogap phase. The latter is therefore not simply a precursor of the former. Looking at high-pressure data, we find that when charge order is suppressed, the superconducting dome in the phase diagram of $YBa_2Cu_3O_y$ is transformed so that it no longer dips but instead now peaks at $p \simeq 0.12$. The fact that in the absence of mutual competition the domes of superconductivity and of charge order both peak at the same doping is strong evidence for the existence of a third phase that competes with both orders at low doping, thereby shaping the phase diagram of cuprates.

PACS numbers: 74.72.Gh, 74.62.Fj, 74.25.Dw

The recent observation of charge density modulations in $YBa_2Cu_3O_y$ (YBCO) [1–4], $La_{2-x}Sr_xCuO_4$ (LSCO) [5], $HgBa_2CuO_{4+\delta}$ [6], and $Bi_2Sr_2CuO_{6+\delta}$ [7] shows that charge-density-wave (CDW) order is a generic tendency of cuprates, not specific to materials such as $La_{2-x}Ba_xCuO_4$ (LBCO), where it has long been known to exist [8]. In Fig. 1, the onset temperature of CDW modulations seen in YBCO by X-ray diffraction, $T_{\rm CDW}$, is plotted as a function of doping [9, 10]. It forms a dome peaked at $p = 0.12$, as does the onset temperature of CDW order seen by NMR (above a threshold magnetic field), $T_{\rm NMR}$ [11]. The Fermi surface of YBCO undergoes a reconstruction, attributed to CDW order, into small electron [12] and hole [13] pockets at low temperature. This process is detected as a downturn in the Hall coefficient $R_{\rm H}(T)$ towards negative values [14], which starts at a temperature $T_{\rm FSR}$ [15]. As seen in Fig. 1, the onset of Fermi-surface reconstruction (FSR), at $T_{\rm FSR}$, also peaks at $p = 0.12$. CDW and FSR also both peak at $p = 0.12$ in $La_{1.8-x}Eu_{0.2}Sr_xCuO_4$ [16, 17].

The striking experimental fact is that the CDW phase in cuprates is peaked at $p = 0.12$. The question is why? Old explanations in terms of a commensurate match of the CDW period with either the lattice or the hole density are no longer viable. Indeed, while in LBCO or LSCO-based materials the CDW incommensurability tracks p and the period becomes nearly commensurate with the lattice at $p \simeq 0.12$, neither of these facts are true for YBCO [9, 10]. For some as yet unknown reason, the conditions for CDW formation in cuprates are most favourable at $p = 0.12$.

CDW order and superconductivity are competing phases. X-ray intensity drops sharply below $T_{\rm c}$ [2, 3],

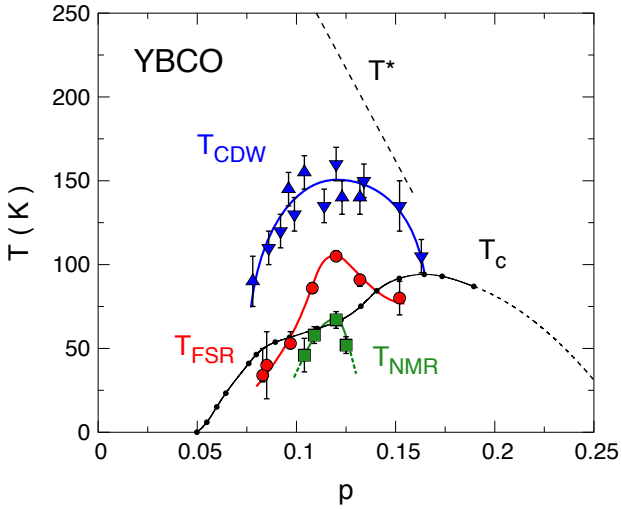


FIG. 1: Temperature-doping phase diagram of YBCO, showing the superconducting phase below $T_{\rm c}$ (black dots [18]) and the onset of charge order seen by NMR, above a threshold magnetic field, below $T_{\rm NMR}$ (green squares [11]). Charge-density modulations are detected by X-ray diffraction below $T_{\rm CDW}$ (up triangles [9]; down triangles [10]). The Fermi surface undergoes a reconstruction seen as a downturn in the Hall coefficient below $T_{\rm FSR}$ (red circles [15]). $T^\star$ marks the onset of the pseudogap phase (dashed line [19, 20]).

showing that superconductivity weakens CDW order in YBCO. Conversely, CDW order weakens superconductivity. This shows up in the doping dependence of the superconducting critical temperature $T_{\rm c}$ and field $H_{\rm c2}$, as a dip in the former (Fig. 1) [18] and a local minimum in the latter [21], both centred at $p = 0.12$, where CDW order is strongest. The dip in $T_{\rm c}$ was shown to scale with

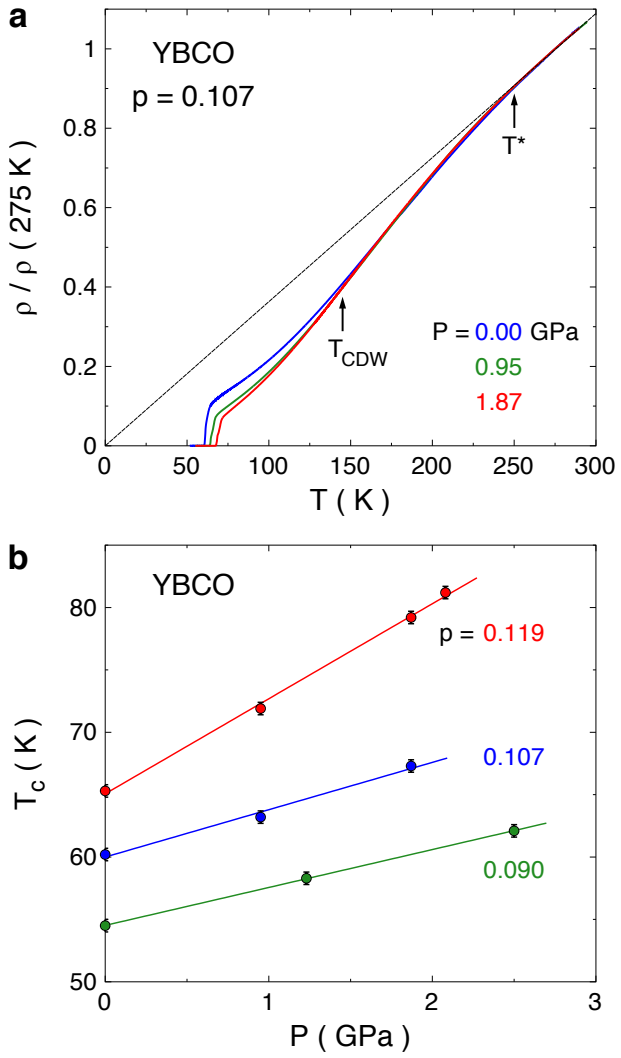


FIG. 2: a) Electrical resistivity $\rho_a(T)$ of YBCO with a doping $p = 0.107$, measured along the a axis of the orthorhombic crystal structure, as a function of temperature, at three pressures as indicated. The curves are normalized to 1.0 at $T = 275$ K (for the unnormalized data, see Fig. S1 of the Supplemental Material [22]). The straight line is a linear fit to the high-temperature data, extended to $T = 0$. $T^\star$ (arrow) marks the onset of the pseudogap phase, defined as the temperature below which $\rho_a(T)$ deviates from its linear dependence at high temperature [19, 20]. T_{CDW} (arrow) is the onset of CDW modulations (Fig. 1). b) Superconducting transition temperature T_c of YBCO as a function of pressure (applied at room temperature), for our three oxygen-ordered crystals, with doping values p as indicated. T_c is obtained from resistivity data in Figs. S1, S2 and S3 of the Supplemental Material.

the onset of FSR, closely linking the two [15]. Application of a magnetic field H restores the CDW amplitude below T_c, while it has no effect above T_c [3]. This shows that one can tune the competition between CDW order and superconductivity by applying a magnetic field.

Here we show that pressure is a second, independent tuning parameter for this competition, which weakens CDW order, with little direct effect on superconductivity, or on the pseudogap phase. By applying large pressures, one can therefore suppress CDW order and obtain the superconducting phase diagram free of competition. Using existing data, we show that under high pressures the dome of T_c is no longer peaked at $p = 0.16$, the usual optimal doping, but at $p \simeq 0.12$. The fact that both CDW order and superconductivity peak at the same doping in the absence of mutual competition reveals that some competing mechanism acts to suppress both below $p \simeq 0.12$. Identifying this mechanism will be key to understanding the cuprate phase diagram.

Methods. – Single crystals of $YBa_2Cu_3O_y$ were prepared as described elsewhere [23], with oxygen content ranging from $y = 6.35$ to $y = 6.998$. The hole concentration (doping) p of each sample is given by its superconducting critical temperature T_c [18]. T_c was determined from transport measurements of the electrical resistance $\rho(T)$ or Nernst signal $N(T)$ as a function of temperature, and defined as the temperature below which ρ and N are zero. The pressure dependence of the a-axis electrical resistivity $\rho_a(T)$ was measured on three single crystals with a high degree of oxygen order: 1) $y = 6.50$, $T_c(0) = 54.5$ K, $p = 0.090$ (ortho-II order); 2) $y = 6.54$, $T_c(0) = 60.2$ K, $p = 0.107$ (ortho-II order); 3) $y = 6.67$, $T_c(0) = 65.3$ K, $p = 0.119$ (ortho-VIII order). Samples were pressurized in a nonmagnetic piston-cylinder clamp cell with a 1/1 mixture of pentane and 3-methyl-1-butanol as the transmitting medium, ensuring a hydrostatic pressure. The magnitude of the applied pressure was determined from the superconducting transition of a lead sample placed inside the cell. Note that pressure can enhance oxygen order in YBCO, and oxygen ordering increases the doping in the CuO_2 planes. To avoid this, one can either apply pressure at temperatures below $\sim$ 200 K [24, 25] or use samples prepared with a high degree of oxygen order. We used oxygen-ordered samples and applied pressure at room temperature. Measurements of $\rho(T)$ and $N(T)$ in a magnetic field $H = 0$ and $H = 15$ T (applied along the c axis of the orthorhombic structure) allowed us to obtain $T_c(H = 0)$ and $T_c(H = 15$ T). The values of y, p, $T_c(H = 0)$ and $T_c(H = 15$ T) for our 13 YBCO samples are listed in Table S1 of the Supplemental Material. This includes a sample with 1.4 % of Ca substitution (at $y \simeq 7$), for which $p = 0.19$.

Sensitivity to pressure. – In Figs. S1, S2 and S3 of the Supplemental Material, the resistivity of our 3 oxygen-ordered YBCO samples is plotted vs temperature, for different values of the applied pressure. The data for $p = 0.107$ are shown in Fig. 2a, normalized at $T = 275$ K. We see that above 150 K, pressure has no effect on the shape of $\rho_a(T)$. The same is true not only in YBCO at the other dopings, but also in $YBa_2Cu_4O_8$ ($p = 0.14$), measured recently up to 10 GPa [26] (see Fig. S4 in the

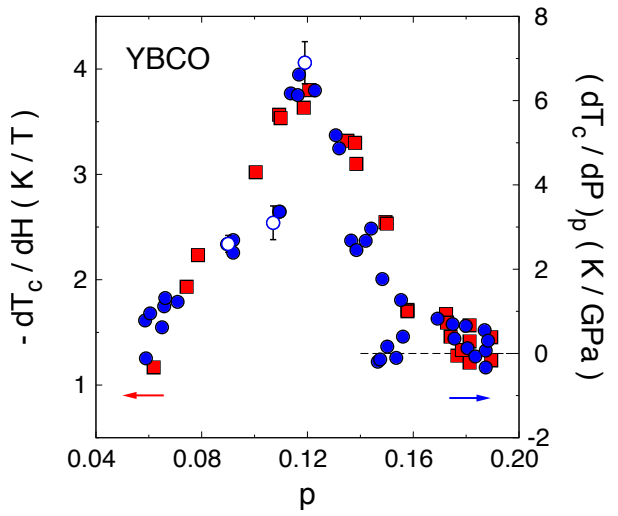


FIG. 3: Sensitivity of T_c in YBCO to pressure P and magnetic field H, as a function of doping p. The former is defined as the amount dT_c by which T_c is increased by the application of a small hydrostatic pressure dP (at constant p), plotted as $(\partial T_c/\partial P)_p$ vs p (blue circles, right axis; Table S2 in the Supplemental Material). Open circles with error bars are from our own data on oxygen-ordered crystals (Fig. 2b); full circles are from published data (Table S2 and Fig. S5 in the Supplemental Material). To get $(\partial T_c/\partial P)_p$, a small doping-dependent correction is applied to the measured dT_c / dP, that accounts for the increase in doping, and hence in T_c, due to pressure (see Supplemental Material). The dashed line marks $(\partial T_c/\partial P)_p = 0$. The sensitivity to field is defined as the amount dT_c by which T_c is reduced by a magnetic field of 15 T : $-\ dT_c/\ dH = [T_c(H = 0) - T_c(H = 15\ \mathrm{T})]/15$ T (red squares, left axis; Table S1 in the Supplemental Material).

Supplemental Material). This shows that the signature of the pseudogap phase in $\rho_a(T)$, namely a downturn below $T^\star$ (Fig. 2a), is unaffected by pressure. We conclude that pressure has little impact on the pseudogap phase of cuprates, at least up to $P \simeq 10$ GPa. We attribute the changes in $\rho_a(T)$ observed below $T_{CDW} \simeq 150$ K (Fig. 2a) to changes in the CDW-induced FSR.

In contrast to $T^\star$, pressure has a large effect on T_c. In Fig. 2b, we plot the pressure dependence of T_c. The slope dT_c/dP has a positive value, of magnitude 3.0 $\pm$ 0.2, 3.5 $\pm$ 0.4, and 7.5 $\pm$ 0.5 K / GPa for $p = 0.090$, 0.107, and 0.119, respectively, in good agreement with published data obtained by applying pressure at low temperature (see Fig. S5 in the Supplemental Material). This confirms that there are no oxygen-ordering effects.

In Fig. 3, we plot our values of dT_c/dP vs p together with a collection of published data, all corrected for the small effect of pressure-induced doping [27, 28] (see Supplemental Material). Both the measured dT_c/dP and the corrected $(\partial T_c/\partial P)_p$ peak sharply at $p = 0.12$ (Fig. S5 of the Supplemental Material), as noted earlier [29]. The dramatic increase in dT_c/dP between $p \simeq 0.11$ and $p \simeq 0.12$ (Fig. 2b), previously detected in thermal expansion measurements at ambient pressure [30], signals a rapid change in the properties of YBCO near $p = 0.12$. Note also that T_c is enhanced by pressure only below $p \simeq 0.16$. Given that CDW order onsets below $p \simeq 0.16$ and peaks at $p = 0.12$ (Fig. 1), we attribute the pressure enhancement of T_c to a suppression of the competing CDW order. This interpretation is confirmed by looking at the effect of a magnetic field, an established tuning parameter for this phase competition.

Sensitivity to field. – The sensitivity of the superconducting transition temperature T_c to a magnetic field H applied along the c axis was studied across the doping range of YBCO, from $p \simeq 0.06$ to $p \simeq 0.2$. Using either resistivity or Nernst data (Figs. S6 and S7 in the Supplemental Material), the amount dT_c by which T_c is reduced when a field of 15 T is applied was measured on 13 different single crystals (Table S1 in the Supplemental Material). The sensitivity to field, defined as $-\ dT_c/dH = [T_c(H = 0) - T_c(H = 15\ \mathrm{T})]/15$ T, is plotted in Fig. 3.

We see that it is small and flat above $p = 0.16$, it rises rapidly below $p = 0.16$, to reach a maximum at $p = 0.12$, and then decreases at lower p. So $-\ dT_c/dH$ vs p peaks at $p = 0.12$. This is not surprising, since we know that H_{c2} vs p has a local minimum at $p \simeq 0.12$ [15, 21]. Note also that T_{CDW} intersects T_c at $p \simeq 0.16$ (Fig. 1), thereby explaining the low sensitivity at $p > 0.16$. All this confirms that superconductivity is weakened when CDW order grows, consistent with the scenario of phase competition discussed above.

Discussion. – In Fig. 3, we see that $\partial T_c/\partial P$ and $-\ \partial T_c/\partial H$ track each other : both are small and flat for $p > 0.16$, both rise rapidly below $p = 0.16$, and both peak at $p = 0.12$. The two sensitivities look so identical as a function of doping because H and P are pure tuning parameters: H does not directly couple to CDW order [3] and P does not directly couple to superconductivity ($\partial T_c/\partial P \sim 0$ at $p > 0.16$). Field and pressure are two complementary parameters with which to tune phase competition between CDW order and superconductivity in YBCO, in opposite directions. This confirms our interpretation that pressure suppresses CDW order in YBCO. Note that X-ray diffraction studies in LBCO at $p = 0.125$ showed directly that CDW order is suppressed by pressure in that material, while T_c rises [31].

We therefore expect that a sufficiently strong pressure will suppress CDW order entirely and reveal the superconducting phase diagram of YBCO free of competition. In Fig. 4, we plot T_c vs p at $P = 2$ GPa and 15 GPa, using data from ref. 25 (reproduced in Fig. S8 of the Supplemental Material). We see that when CDW order is removed, the superconducting phase in the temperature-doping diagram of YBCO is transformed in two important ways. First, the dip at $p \simeq 0.12$ goes away, so that by $P = 15$ GPa, T_c forms a dome peaked at $p \simeq 0.13$. Secondly, the foot of the dome at low doping moves up,

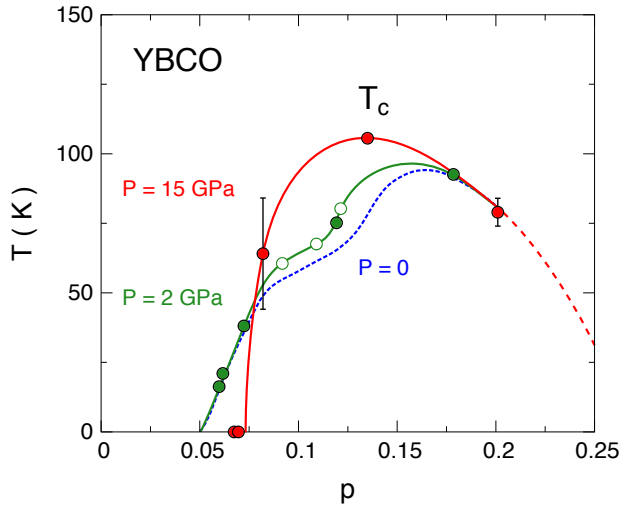


FIG. 4: Superconducting phase diagram of YBCO, showing T_c at ambient pressure ($P = 0$, dotted blue line; Fig. 1 [18]) and at $P = 2$ GPa (green circles; from our 3 samples, open circles (Fig. 2b); from the 5 samples of ref. 25, full circles). T_c measured at, or extrapolated to, $P = 15$ GPa is shown as red circles (from ref. 25; see Fig. S8 in the Supplemental Material). The doping value for each data point includes the effect of pressure (see Supplemental Material). The red and green lines are a guide to the eye.

from $p = 0.05$ to $p \simeq 0.075$. As a result, the fall of T_c with decreasing p is much faster than it was at ambient pressure (Fig. 4). At $P = 0$, T_c falls below $p \simeq 0.16$ because a competing phase of CDW order sets in below a $T = 0$ critical point at $p \simeq 0.18$ [21, 32, 33]. At $P = 15$ GPa, this CDW critical point is removed, yet T_c is still a dome, now falling below $p \simeq 0.13$. What competing phase, resistant to pressure, is causing that fall? Let us mention two possible scenarios.

The first scenario is spin order. In YBCO at ambient pressure, long-range antiferromagnetic order exists up to $p = 0.05$ and short-range incommensurate spin-density-wave (SDW) correlations extend up to $p \simeq 0.08$ [34]. CDW, SDW and superconducting phases all compete with each other [35]. By suppressing CDW order, pressure could strengthen SDW order, extend its range up to higher p, and stiffen its competing effect on superconductivity at low doping.

A second scenario for a competition that persists at high pressure is the pseudogap phase. In particular, the pseudogap due to strong correlations associated with the Mott insulator is known to compete with superconductivity [36, 37], and to produce a dome of T_c vs p [38]. It remains to be seen where in doping the peak in T_c lies with respect to the $T^\star$ line and the underlying critical point for the transition from Fermi-liquid phase at high p to pseudogap phase at low p [39, 40].

In any scenario, two questions must be addressed: Why a dome of CDW order peaked at $p \simeq 0.12$? Why does pressure have such a strong detrimental effect on CDW order, while it has little direct effect on either superconductivity or the pseudogap phase?

Summary. – Over the years, the numerous studies of the effect of pressure on T_c in YBCO have collectively revealed a complex behavior that has remained a mystery. A crucial piece of information that had been missing until recently to make sense of the apparent complexity is the existence of a dome of CDW order in YBCO. Here we showed that magnetic field H and pressure P shift T_c in the same way as a function of doping, but in opposite directions, and conclude that H and P are two independent parameters with which to tune the competition between superconductivity and CDW order in YBCO: H suppresses the former and P suppresses the latter. This is most likely why the record T_c in cuprate superconductors was reached by applying pressure [41]. In YBCO at high pressures, when CDW order is removed, the superconducting dome of T_c vs p is seen to peak at $p \simeq 0.12$, revealing that another competing mechanism is at play at low doping. We mention that this could be a phase of spin order or the pseudogap phase, amongst other possibilities, and propose that one way to discriminate between the various scenarios is to ask why would CDW order also happen to peak at $p \simeq 0.12$, a universal fact of cuprate superconductors.

Acknowledgements. – We thank J. Corbin, M.-È. Delage, G. Grissonnanche, E. Hassinger, F. Laliberté, S. René de Cotret, F F. Tafti for their assistance with the experiments, and B. J. Ramshaw for his assistance with sample preparation. L.T. thanks ESPCI-ParisTech, École Polytechnique, Université Paris-Sud, CEA-Saclay and the Collège de France for their hospitality and support, and the LabEx PALM for its support, while this article was written. L.T. acknowledges support from the Canadian Institute for Advanced Research (CIFAR) and funding from the National Science and Engineering Research Council of Canada (NSERC), the Fonds de recherche du Québec - Nature et Technologies (FRQNT), the Canada Foundation for Innovation (CFI) and a Canada Research Chair.

* Present address: Laboratoire National des Champs Magnétiques Intenses (CNRS, INSA, UJF, UPS), 31400 Toulouse, France.
† Electronic address: louis.taillefer@usherbrooke.ca

[1] T. Wu, H. Mayaffre, S. Krämer, M. Horvatić, C. Berthier, W. N. Hardy, R. Liang, D. A. Bonn, and M.-H. Julien, Nature **477**, 191 (2011).
[2] G. Ghiringhelli, M. Le Tacon, M. Minola, S. Blanco-Canosa, C. Mazzoli, N. B. Brookes, G. M. De Luca, A. Frano, D. G. Hawthorn, F. He, *et al.*, Science **337**, 821 (2012) .
[3] J. Chang, E. Blackburn, A. T. Holmes, N. B. Christensen, J. Larsen, J. Mesot, R. Liang, D. A. Bonn, W. N.

Hardy, A. Watenphul, *et al.*, Nat. Phys. **8**, 871 (2012).
[4] A. J. Achkar, R. Sutarto, X. Mao, F. He, A. Frano, S. Blanco-Canosa, M. Le Tacon, G. Ghiringhelli, L. Braicovich, M. Minola, *et al.*, Nat. Phys. **8**, 871 (2012).
[5] T. P. Croft, C. Lester, M. S. Senn, A. Bombardi, and S. M. Hayden, Phys. Rev. Lett. **109**, 167001 (2012).
[6] W. Tabis, Y. Li, M. Le Tacon, L. Braicovich, A. Kreyssig, M. Minola, G. Dellea, E. Weschke, M. J. Veit, M. Ramazanoglu, *et al.*, Phys. Rev. B **89**, 224513 (2014).
[7] R. Comin, A. Frano, M. M. Yee, Y. Yoshida, H. Eisaki, E. Schierle, E. Weschke, R. Sutarto, F. He, A. Soumyanarayanan, *et al.*, Science **343**, 390 (2014).
[8] J. M. Tranquada, B. J. Sternlieb, J. D. Axe, Y. Nakamura, and S. Uchida, Nature **375**, 561 (1995)
[9] M. Hücker, N. B. Christensen, A. T. Holmes, E. Blackburn, E. M. Forgan, R. Liang, D. A. Bonn, W. N. Hardy, O. Gutowski, M. v. Zimmermann, *et al.*, Phys. Rev. B **90**, 054514 (2014).
[10] S. Blanco-Canosa, A. Frano, E. Schierle, J. Porras, T. Loew, M. Minola, M. Bluschke, E. Weschke, B. Keimer, and M. Le Tacon, Phys. Rev. B **90**, 054513 (2014).
[11] T. Wu, H. Mayaffre, S. Krämer, M. Horvatić, C. Berthier, P. L. Kuhns, A. P. Reyes, R. Liang, W. N. Hardy, D. A. Bonn, *et al.*, Nat. Commun. **4**, 2113 (2013) .
[12] N. Doiron-Leyraud, C. Proust, D. LeBoeuf, J. Levallois, J.-B. Bonnemaison, R. Liang, D. A. Bonn, W. N. Hardy, and L. Taillefer, Nature **447**, 565 (2007).
[13] N. Doiron-Leyraud, S. Badoux, S. René de Cotret, S. Lepault, D. LeBoeuf, F. Laliberté, E. Hassinger, B. J. Ramshaw, D. A. Bonn, W. N. Hardy, *et al.*, Nat. Commun. **6**, 6034 (2015).
[14] D. LeBoeuf, N. Doiron-Leyraud, J. Levallois, R. Daou, J.-B. Bonnemaison, N. E. Hussey, L. Balicas, B. J. Ramshaw, R. Liang, D. A. Bonn, *et al.*, Nature **450**, 533 (2007).
[15] D. LeBoeuf, N. Doiron-Leyraud, B. Vignolle, M. Sutherland, B. J. Ramshaw, J. Levallois, R. Daou, F. Laliberté, O. Cyr-Choinière, J. Chang, *et al.*, Phys. Rev. B **83**, 054506 (2011).
[16] J. Fink, V. Soltwisch, J. Geck, E. Schierle, E. Weschke, and B. Büchner, Phys. Rev. B **83**, 092503 (2011).
[17] F. Laliberté, J. Chang, N. Doiron-Leyraud, E. Hassinger, R. Daou, M. Rondeau, B. J. Ramshaw, R. Liang, D. A. Bonn, W. N. Hardy, *et al.*, Nat. Commun. **2**, 432 (2011).
[18] R. Liang, D. A. Bonn, and W. N. Hardy, Phys. Rev. B **73**, 180505(R) (2006).
[19] Y. Ando, S. Komiya, K. Segawa, S. Ono, and Y. Kurita, Phys. Rev. Lett. **93**, 267001 (2004).
[20] R. Daou, J. Chang, D. LeBoeuf, O. Cyr-Choinière, F. Laliberté, N. Doiron-Leyraud, B. J. Ramshaw, R. Liang, D. A. Bonn, W. N. Hardy, *et al.*, Nature **463**, 519 (2010).
[21] G. Grissonnanche, O. Cyr-Choinière, F. Laliberté, S. René de Cotret, A. Juneau-Fecteau, S. Dufour-Beauséjour, M.-E. Delage, D. LeBoeuf, J. Chang, B. J. Ramshaw, *et al.*, Nat. Commun. **5**, 3280 (2014).
[22] See Supplemental Material at [URL] for Figs. S1 to S8 and Tables S1 and S2.
[23] R. Liang, D. A. Bonn, and W. N. Hardy, Philos. Mag. **92**, 2563 (2012).
[24] S. Sadewasser, Y. Wang, J. S. Schilling, H. Zheng, A. P. Paulikas, and B. W. Veal, Phys. Rev. B **56**, 14168 (1997).
[25] S. Sadewasser, J. S. Schilling, A. P. Paulikas, and B. W. Veal, Phys. Rev. B **61**, 741 (2000).
[26] A. Nakayama, Y. Onda, S. Yamada, H. Fujihisa, M. Sakata, Y. Nakamoto, K. Shimizu, S. Nakano, A. Ohmura, F. Ishikawa, *et al.*, J. Phys. Soc. Jpn. **83**, 093601 (2014).
[27] C. C. Almasan, S. H. Han, B. W. Lee, L. M. Paulius, M. B. Maple, B. W. Veal, J. W. Downey, A. P. Paulikas, Z. Fisk, and J. E. Schirber, Phys. Rev. Lett. **69**, 680 (1992).
[28] J. J. Neumeier and H. A. Zimmermann, Phys. Rev. B **47**, 8385 (1993).
[29] R. Benischke, T. Weber, W. H. Fietz, J. Metzger, K. Grube, T. Wolf, and H. Wühl, Physica C **203**, 293 (1992).
[30] O. Kraut, C. Meingast, G. Bräuchle, H. Claus, A. Erb, G. Müller-Vogt, and H. Wühl, Physica C **205**, 139 (1993).
[31] M. Hücker, M. v. Zimmermann, M. Debessai, J. S. Schilling, J. M. Tranquada, and G. D. Gu, Phys. Rev. Lett. **104**, 057004 (2010).
[32] J. Luo, J. Loram, J. Cooper, and J. Tallon, Physica C **341–348**, 1837 (2000).
[33] B. J. Ramshaw, S. E. Sebastian, R. D. McDonald, J. Day, B. Tam, Z. Zhu, J. B. Betts, R. Liang, D. A. Bonn, W. N. Hardy, *et al.*, arXiv:1409.3990 (2014).
[34] D. Haug, V. Hinkov, Y. Sidis, P. Bourges, N. B. Christensen, A. Ivanov, T. Keller, C. T. Lin, and B. Keimer, New J. Phys. **12**, 105006 (2010).
[35] S. Blanco-Canosa, A. Frano, T. Loew, Y. Lu, J. Porras, G. Ghiringhelli, M. Minola, C. Mazzoli, L. Braicovich, E. Schierle, *et al.*, Phys. Rev. Lett. **110**, 187001 (2013).
[36] A. Georges, G. Kotliar, W. Krauth, and M. J. Rozenberg, Rev. Mod. Phys. **68**, 13 (1996).
[37] A.-M. S. Tremblay, in *Emergent Phenomena in Correlated Matter Modeling and Simulation*, Vol. 3, edited by E. Pavarini, E. Koch, and U. Schollwöck (Forschungszentrum Jülich, 2013) Chap. 10.
[38] E. Gull, O. Parcollet, and A. J. Millis, Phys. Rev. Lett. **110**, 216405 (2013).
[39] P. Werner, E. Gull, O. Parcollet, and A. J. Millis, Phys. Rev. B **80**, 045120 (2009).
[40] G. Sordi, P. Sémon, K. Haule, and A.-M. S. Tremblay, Sci. Rep. **2**, 547 (2012).
[41] L. Gao, Y. Y. Xue, F. Chen, Q. Xiong, R. L. Meng, D. Ramirez, C. W. Chu, J. H. Eggert, and H. K. Mao, Phys. Rev. B **50**, 4260 (1994).

SUPPLEMENTAL MATERIAL

Suppression of charge order by pressure in the cuprate superconductor $YBa_2Cu_3O_y$: Restoring the full superconducting dome

This Supplemental Material file contains two tables, eight figures and a discussion about the doping effect of pressure in YBCO. Tables S1 and S2 present the values of the data points plotted in Fig. 3. Figs. S1 to S4 plot raw and normalized resistivity curves of some YBCO samples under pressure, similar to Fig. 2a. Fig. S5 presents the extracted values of dT_c/dP from references in the literature and the corresponding corrected values (plotted in Fig. 3). Figs. S6 and S7 plot raw resistivity and Nernst curves at $H = 15$ T, giving $T_c(H = 15$ T) of Table S1. Fig. S8 shows published curves of pressure dependence of T_c in YBCO from ref. [25], used in Fig. 4.

p	y	T_c (0) (K)	T_c (15T) (K)	ΔT_c / 15 (K / T)
0.062	6.35	19.5	2.0	1.17
0.074	6.45	39.5	10.5	1.93
0.079	6.45	45.0	11.5	2.23
0.100	6.49	57.8	12.5	3.02
0.109	6.54	61.3	7.8	3.57
0.110	6.54	61.5	8.5	3.53
0.119	6.67	65.0	10.5	3.63
0.121	6.67	66.0	9.0	3.80
0.135	6.80	78.5	28.7	3.32
0.138	6.80	82.0	32.5	3.30
0.139	6.80	82.5	36.0	3.10
0.150	6.86	90.8	52.6	2.55
0.150	6.86	91.0	53.0	2.53
0.158	6.92	93.5	68.0	1.70
0.158	6.92	93.5	67.8	1.71
0.172	6.95	93.1	68.0	1.67
0.173	6.99	93.0	69.1	1.59
0.174	6.95	92.7	70.8	1.46
0.177	6.97	92.0	72.8	1.28
0.178	6.97	91.5	71.5	1.33
0.181	6.998	90.5	72.3	1.21
0.181	6.998	90.5	69.3	1.41
0.181	6.998	90.5	67.0	1.57
0.190	Ca1.4%	87.0	65.2	1.45
0.190	Ca1.4%	87.0	68.5	1.23

TABLE S1: Characteristics of the 13 YBCO samples whose sensitivity of T_c to field is plotted in Fig. 3, labelled by their oxygen content y: doping p, zero-resistance T_c at $H = 0$ and $H = 15$ T, from resistivity (Fig. S6) or Nernst (Fig. S7) data. $\Delta T_c = T_c(H = 0) - T_c(H = 15$ T); $-dT_c/dH = \Delta T_c/15$ T. The numbers in the last column are plotted as red squares in Fig. 3.

References for data in Table S2 :

C. C. Almasan, S. H. Han, B. W. Lee, L. M. Paulius, M. B. Maple, B. W. Veal, J. W. Downey, A. P. Paulikas, Z. Fisk, and J. E. Schirber, Phys. Rev. Lett. **69**, 680 (1992).

R. Benischke, T. Weber, W. H. Fietz, J. Metzger, K. Grube, T. Wolf, and H. Wühl, Physica C **203**, 293 (1992).

W. H. Fietz, R. Quenzel, K. Grube, J. Metzger, T. Weber, and H. A. Ludwig, Physica C **235-240**, 1785 (1994).

W. H. Fietz, R. Quenzel, H. A. Ludwig, K. Grube, S. I. Schlachter, F. W. Hornung, T. Wolf, A. Erb, M. Kläser, and G. Müller-Vogt, Physica C **270**, 258 (1996).

S. Klotz, W. Reith, and J. S. Schilling, Physica C **172**, 423 (1991).

R. Lortz, T. Tomita, Y. Wang, A. Junod, J. S. Schilling, T. Masui, and S. Tajima, Physica C **434**, 194 (2006).

S. Sadewasser, J. S. Schilling, A. P. Paulikas, and B. W. Veal, Phys. Rev. B **61**, 741 (2000).

V. G. Tissen, Y. Wang, A. P. Paulikas, B. W. Veal and J. S. Schilling, Physica C **316**, 21 (1999).

S. W. Tozer, J. L. Koston, and E. M. McCarron III, Phys. Rev. B **47**, 8089 (1993).

K. Yoshida, A. I. Rykov, S. Tajima, and I. Terasaki, Phys. Rev. B **60**, R15035 (1999).

$T_c(0)$	p	dT_c/dP (K / GPa)	$(\partial T_c/\partial p)_P$ (K / hole)	$(\partial T_c/\partial P)_p$ (K / GPa)	Reference
14.0	0.059	1.1	2064.32	-0.1 ± 0.1	Tissen *et al.* 1999
13.5	0.059	2.0	2079.08	0.8 ± 0.1	Sadewasser *et al.* 2000
17.1	0.061	2.1	1901.22	1.0 ± 0.2	Sadewasser *et al.* 2000
25.0	0.065	1.7	1661.15	0.6 ± 0.3	Fietz *et al.* 1996
26.4	0.066	2.2	1644.39	1.1 ± 0.3	Fietz *et al.* 1996
27.1	0.066	2.4	1636.17	1.3 ± 0.3	Fietz *et al.* 1996
34.4	0.071	2.3	1514.45	1.2 ± 0.1	Sadewasser *et al.* 2000
54.2	0.090	3.0	453.84	2.6 ± 0.2	Benischke *et al.* 1992
54.5	0.090	3.0	428.50	2.6 ± 0.2	This work
55.1	0.092	2.7	337.67	2.4 ± 0.3	Fietz *et al.* 1996
55.1	0.092	3.0	337.67	2.7 ± 0.3	Fietz *et al.* 1996
60.2	0.107	3.5	406.50	3.1 ± 0.4	This work
61.3	0.109	3.8	398.10	3.4 ± 0.2	Benischke *et al.* 1992
61.4	0.110	3.8	396.10	3.4 ± 0.2	Benischke *et al.* 1992
63.0	0.114	6.6	377.22	6.2 ± 0.3	Fietz *et al.* 1996
64.0	0.116	6.6	403.97	6.1 ± 0.3	Fietz *et al.* 1996
64.2	0.117	7.1	412.42	6.6 ± 0.2	Sadewasser *et al.* 2000
65.3	0.119	7.2	467.50	6.9 ± 0.5	This work
67.2	0.123	7.0	616.06	6.2 ± 0.2	Benischke *et al.* 1992
73.6	0.131	6.5	1012.29	5.2 ± 0.2	Benischke *et al.* 1992
75.0	0.132	6.3	1086.33	4.9 ± 0.2	Benischke *et al.* 1992
80.2	0.137	4.3	1187.43	2.7 ± 0.1	Almasan *et al.* 1992
82.5	0.139	4.0	1115.16	2.5 ± 0.1	Almasan *et al.* 1992
86.0	0.142	3.9	864.92	2.7 ± 0.2	Benischke *et al.* 1992
87.7	0.144	4.0	718.94	3.0 ± 0.1	Almasan *et al.* 1992
89.3	0.147	0.7	576.82	-0.2± 0.2	Klotz *et al.* 1991
89.8	0.148	0.6	531.21	-0.1 ± 0.2	Tozer *et al.* 1993
90.2	0.148	2.5	495.32	1.8 ± 0.2	Benischke *et al.* 1992
91.1	0.150	0.8	423.91	0.2 ± 0.1	Fietz *et al.* 1994
92.4	0.154	0.4	328.33	-0.10 ± 0.08	Benischke *et al.* 1992
92.9	0.155	1.7	277.42	1.3 ± 0.1	Almasan *et al.* 1992
93.1	0.156	0.8	257.46	0.4 ± 0.1	Yoshida *et al.* 1999
93.7	0.169	0.6	-157.27	0.83 ± 0.06	Almasan *et al.* 1992
92.5	0.175	0.2	-259.58	0.69 ± 0.06	Sadewasser *et al.* 2000
92.3	0.176	-0.1	-269.86	0.35 ± 0.08	Fietz *et al.* 1996
91.0	0.180	0.05	-335.27	0.65 ± 0.09	Fietz *et al.* 1994
90.8	0.181	-0.5	-346.04	0.1 ± 0.1	Fietz *et al.* 1994
89.7	0.184	-0.8	-396.45	-0.1 ± 0.1	Fietz *et al.* 1994
88.2	0.187	-0.3	-455.77	0.6 ± 0.1	Yoshida *et al.* 1999
88.0	0.187	-0.8	-462.91	0.1 ± 0.1	Fietz *et al.* 1994
88.0	0.187	-1.2	-462.91	-0.33 ± 0.03	Lortz *et al.* 2006
87.6	0.188	-0.6	-479.67	0.3 ± 0.1	Fietz *et al.* 1994

TABLE S2: Characteristics of all samples whose sensitivity of T_c to pressure is plotted in Fig. 3. Zero-resistance T_c at ambient pressure ($P = 0$), doping p, measured initial slope dT_c/dP. $(\partial T_c/\partial P)_p$ corresponds to the measured dT_c/dP corrected for the doping effect of pressure (see Section "Doping effect of pressure in YBCO" below). In the 4th column, we list the term $(\partial T_c/\partial p)_P$ that goes into this correction. The last column gives the reference for the data, by name of first author - year (see list below). Our own three oxygen-ordered samples are identified as "This work".

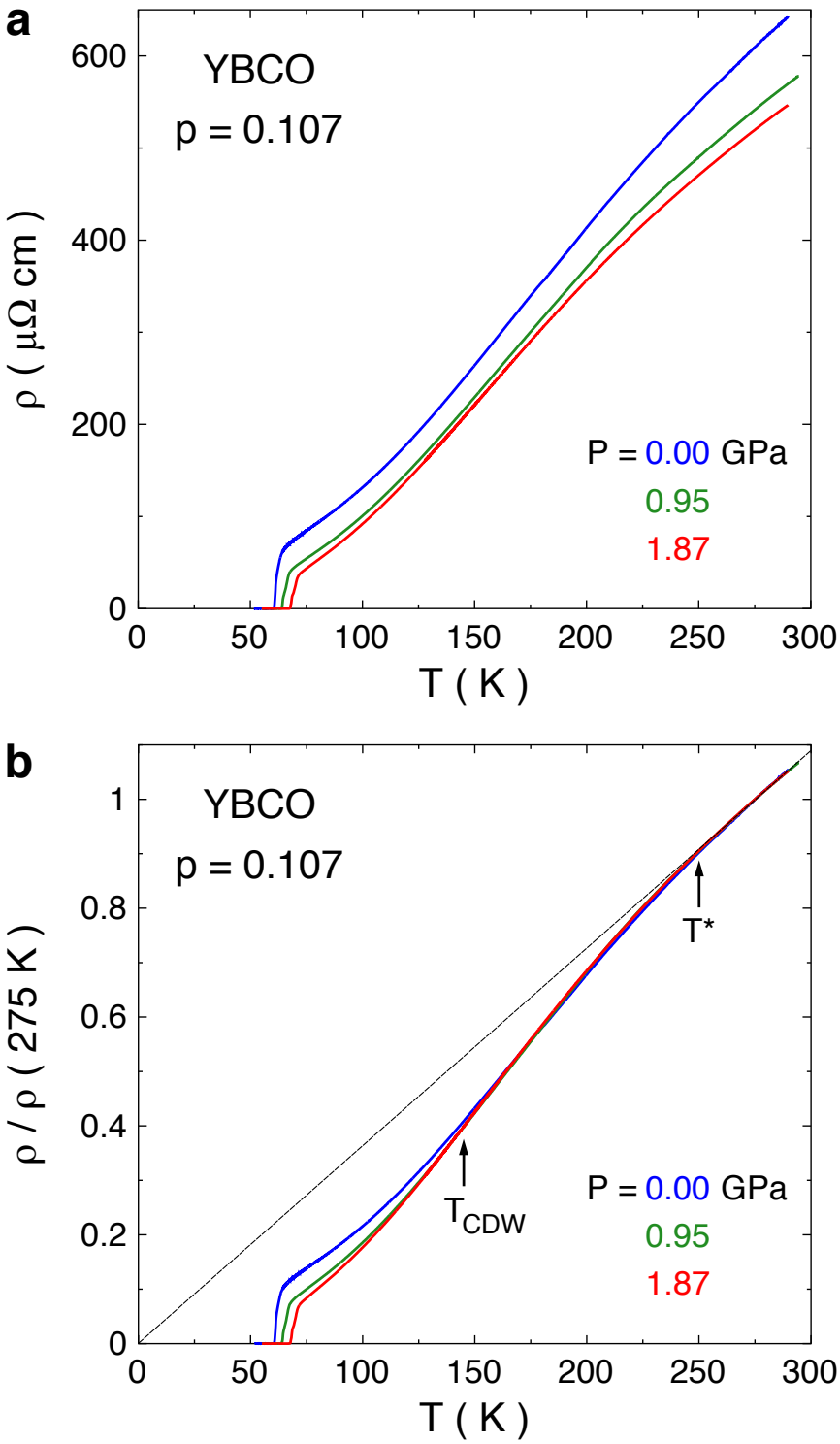


FIG. S1: Resistivity of YBCO at $p = 0.107$. Electrical resistivity $\rho_a(T)$ of YBCO sample with $y = 6.54$ ($T_c = 60.2$ K, $p = 0.107$) and a high degree of oxygen order, measured as a function of temperature for a current along the a axis of the orthorhombic structure, at 3 different pressures as indicated. **a)** Raw data. **b)** Same data as in panel a), but normalized to unity at $T = 275$ K (same as Fig. 2a). The straight line is a linear fit to the data at high temperature, extrapolated to $T = 0$. The pseudogap temperature T^*is defined as the temperature below which $\rho_a(T)$ deviates from its linear dependence at high temperature [19, 20]. T_{CDW} marks the onset of CDW modulations seen in X-ray diffraction at that doping (arrow; see Fig. 1).

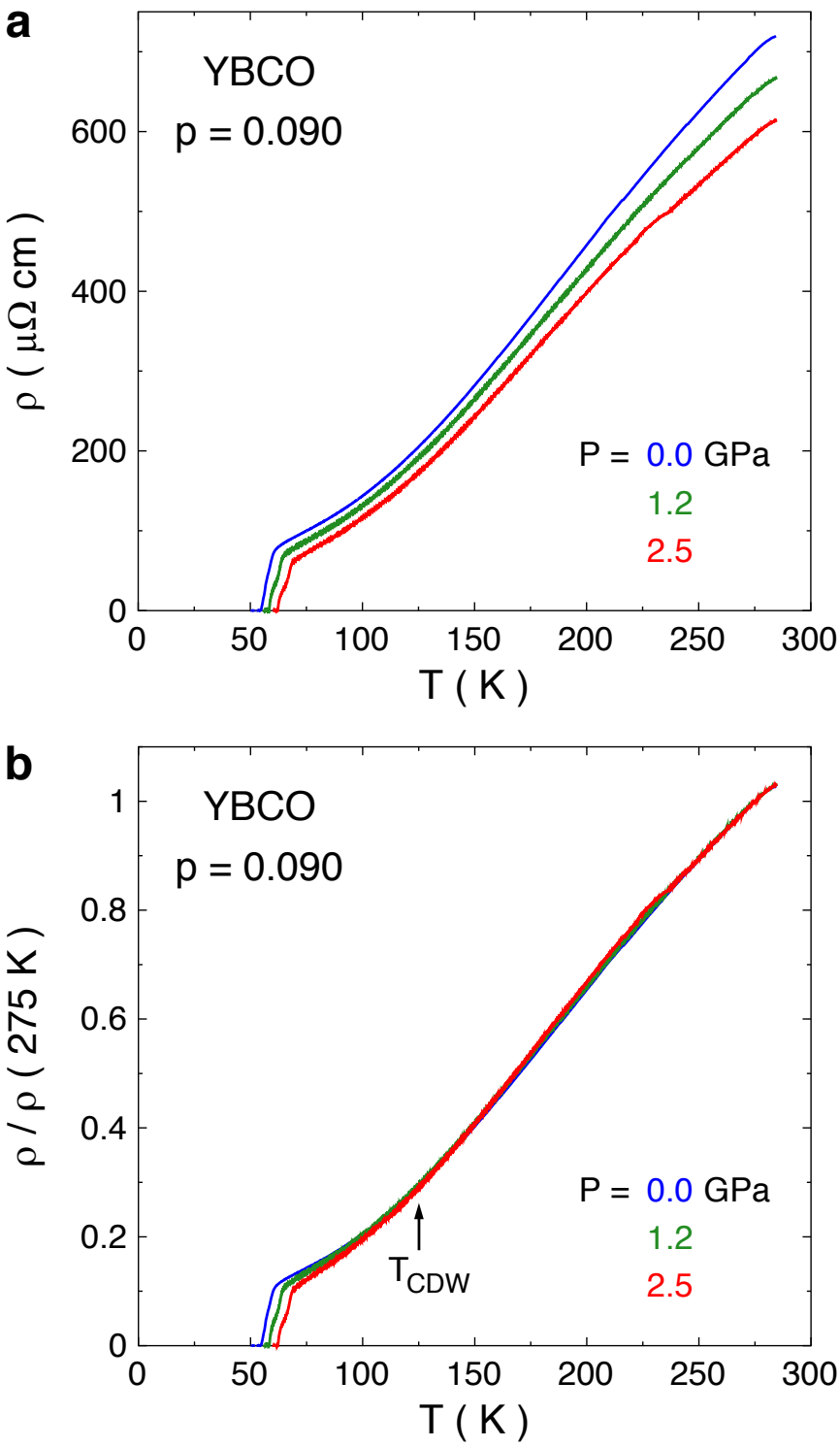


FIG. S2: Resistivity of YBCO at $p = 0.090$. Same as in Fig. S1, but for our YBCO sample with $y = 6.50$ ($T_c = 54.5$ K, $p = 0.090$). Note that $T^\star > 300$ K at this doping [19].

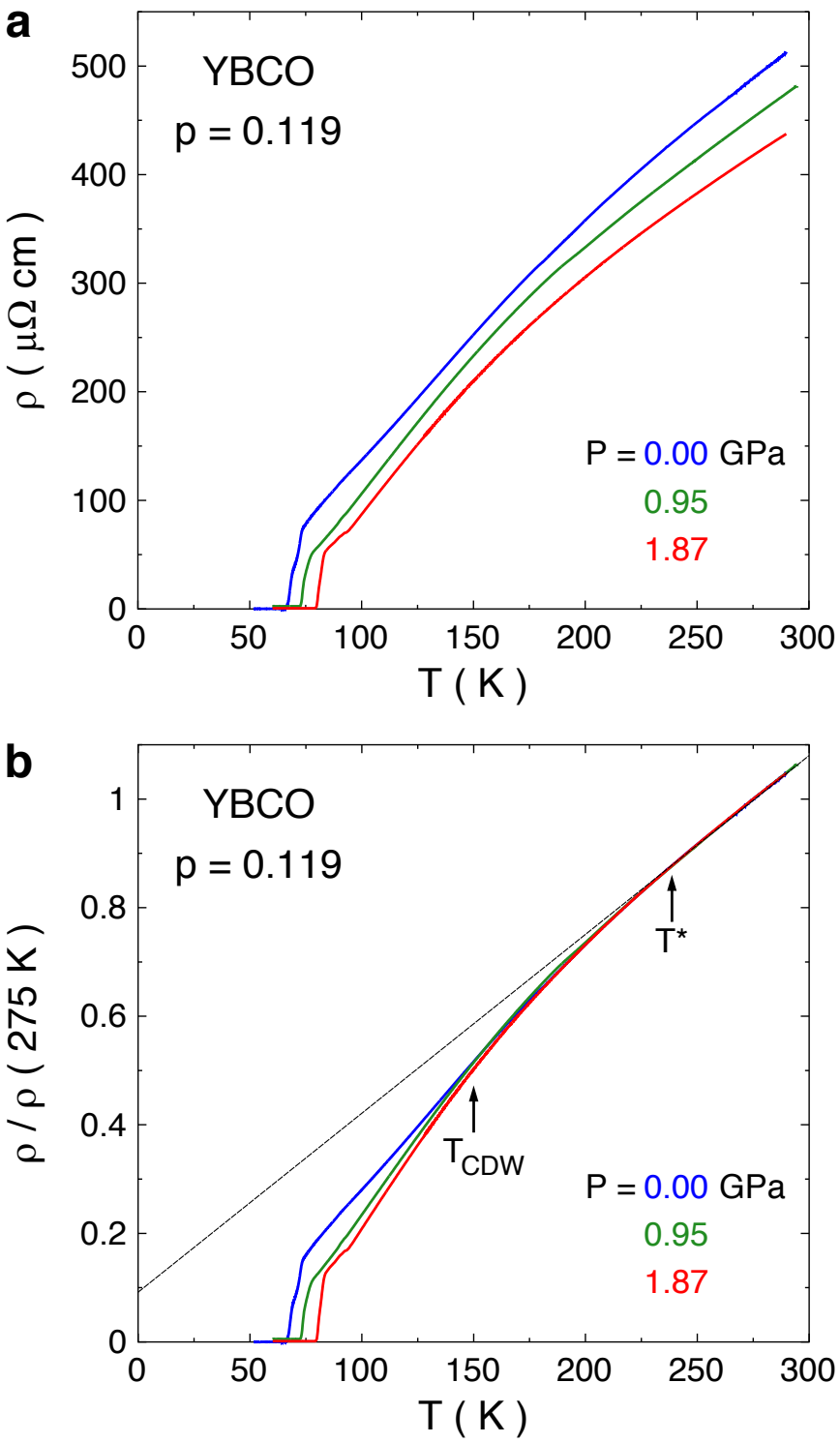


FIG. S3: Resistivity of YBCO at $p = 0.119$. Same as in Fig. S1, but for our YBCO sample with $y = 6.67$ ($T_c = 65.3$ K, $p = 0.119$).

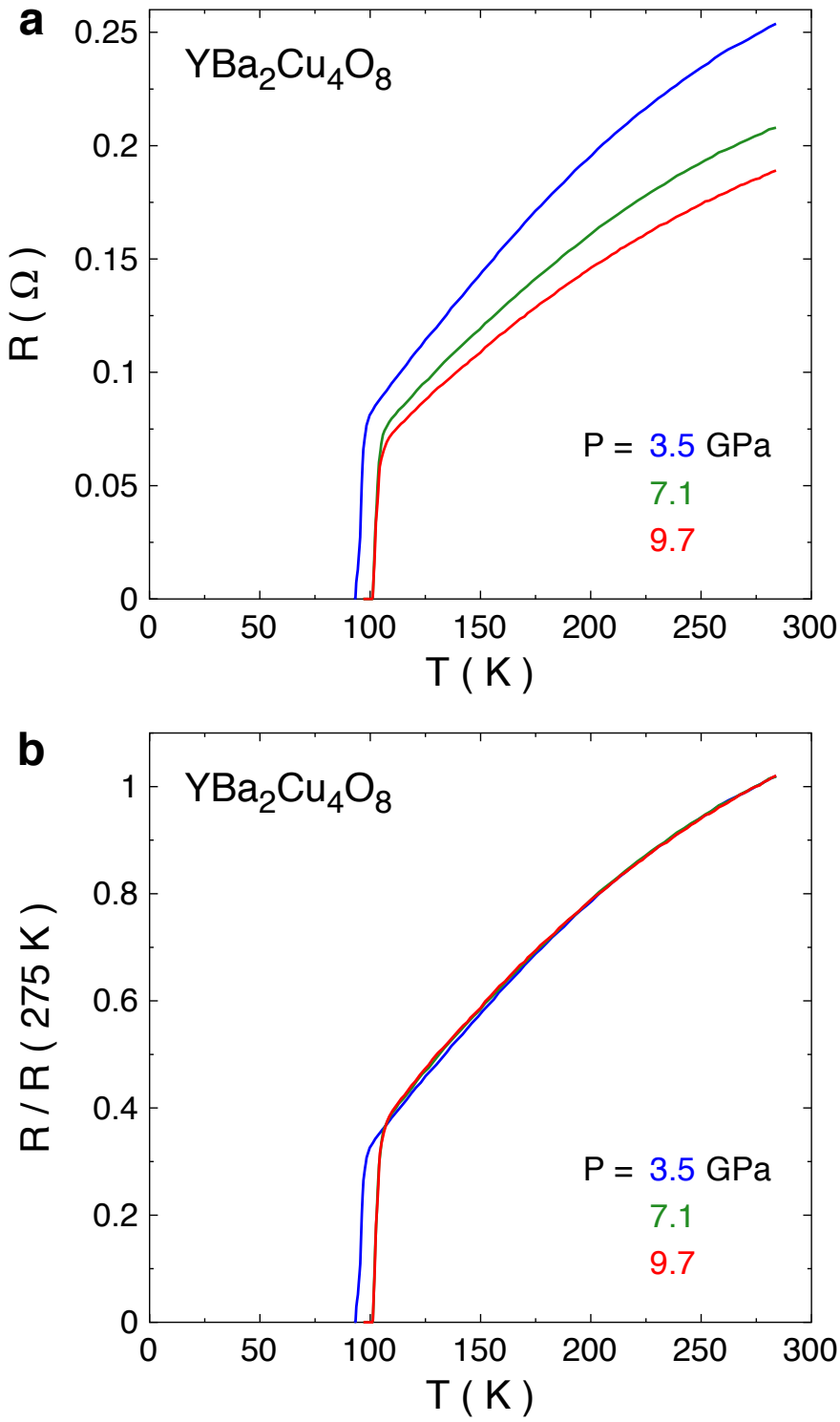


FIG. S4: Resistance of $YBa_2Cu_4O_8$. Electrical resistance of $YBa_2Cu_4O_8$, a stoichiometric underdoped cuprate with perfect oxygen order (T_c = 80 K, $p = 0.14$), reproduced from ref. [26]. The data were taken as a function of temperature for a current along the a axis of the orthorhombic structure, at 3 different pressures [26], as indicated. **a)** Raw data. **b)** Same data as in panel a), but normalized to unity at $T = 275$ K. There is no change in the shape of $\rho_a(T)$ up to 10 GPa.

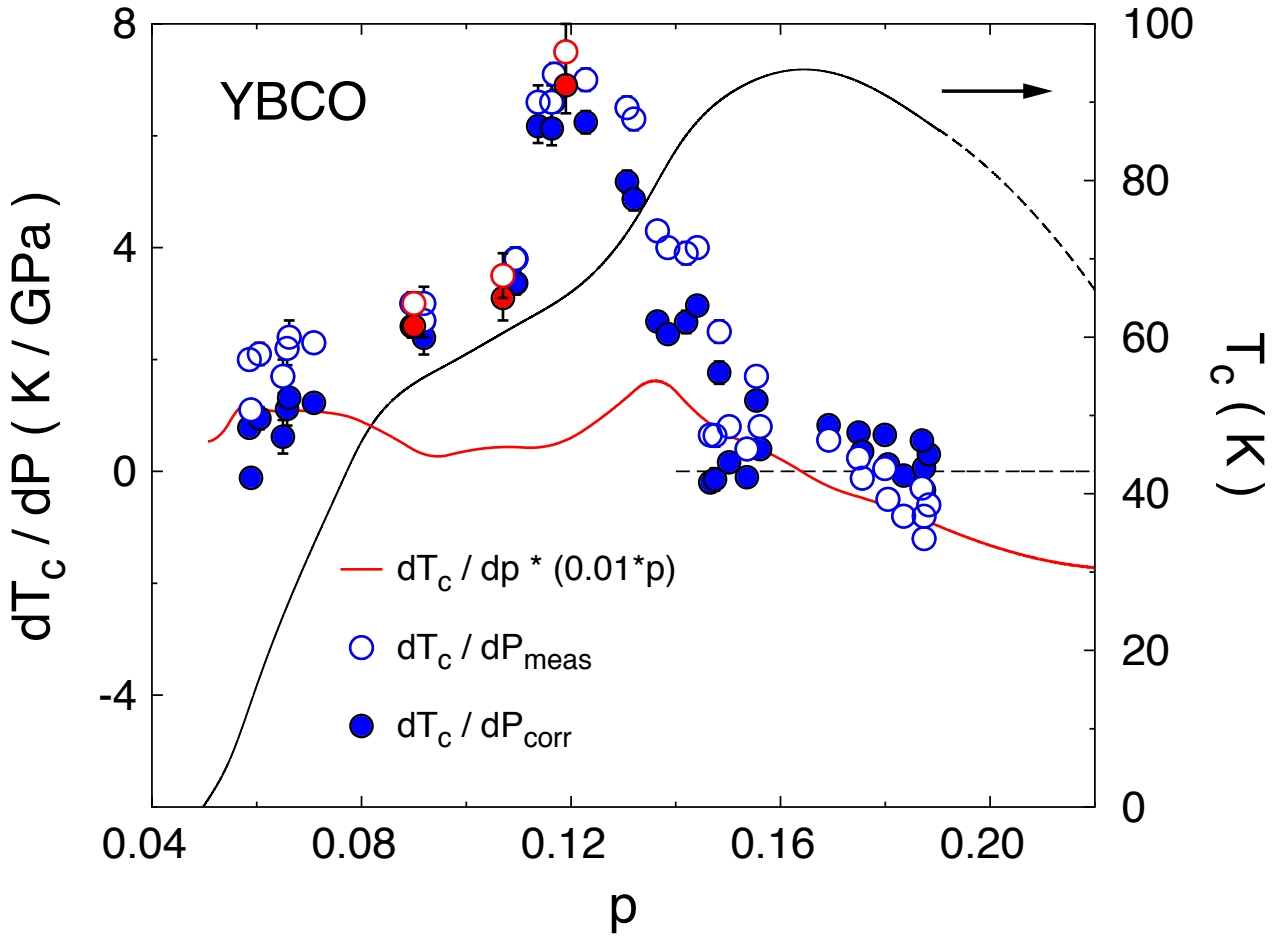


FIG. S5: Sensitivity of T_c to pressure P in YBCO, defined as dT_c/dP, the initial slope in the T_c vs P dependence, as a function of doping p. The data points come from the literature (blue circles; Table S2 and references below it) and from our own measurements (red circles with error bars; Figs. S1, S2, S3). Two quantities are plotted: 1) the measured values of dT_c/dP (labelled $(dT_c/dP)_{\rm meas}$; open circles); 2) the corrected values (labelled $(dT_c/dP)_{\rm corr}$; full circles). The corrected data are obtained via $(dT_c/dP)_{\rm corr} = (\partial T_c/\partial P)_p = (dT_c/dP)_{\rm meas} - 0.01\,p\,(dT_c/dp)$ (see Table S2 and section below). The red line is the magnitude of the correction, with $(\partial T_c/\partial p)_P$ being the derivative of the T_c vs p curve (black line; right axis). The horizontal dashed line marks $(dT_c/dP)_{\rm corr} = 0$.

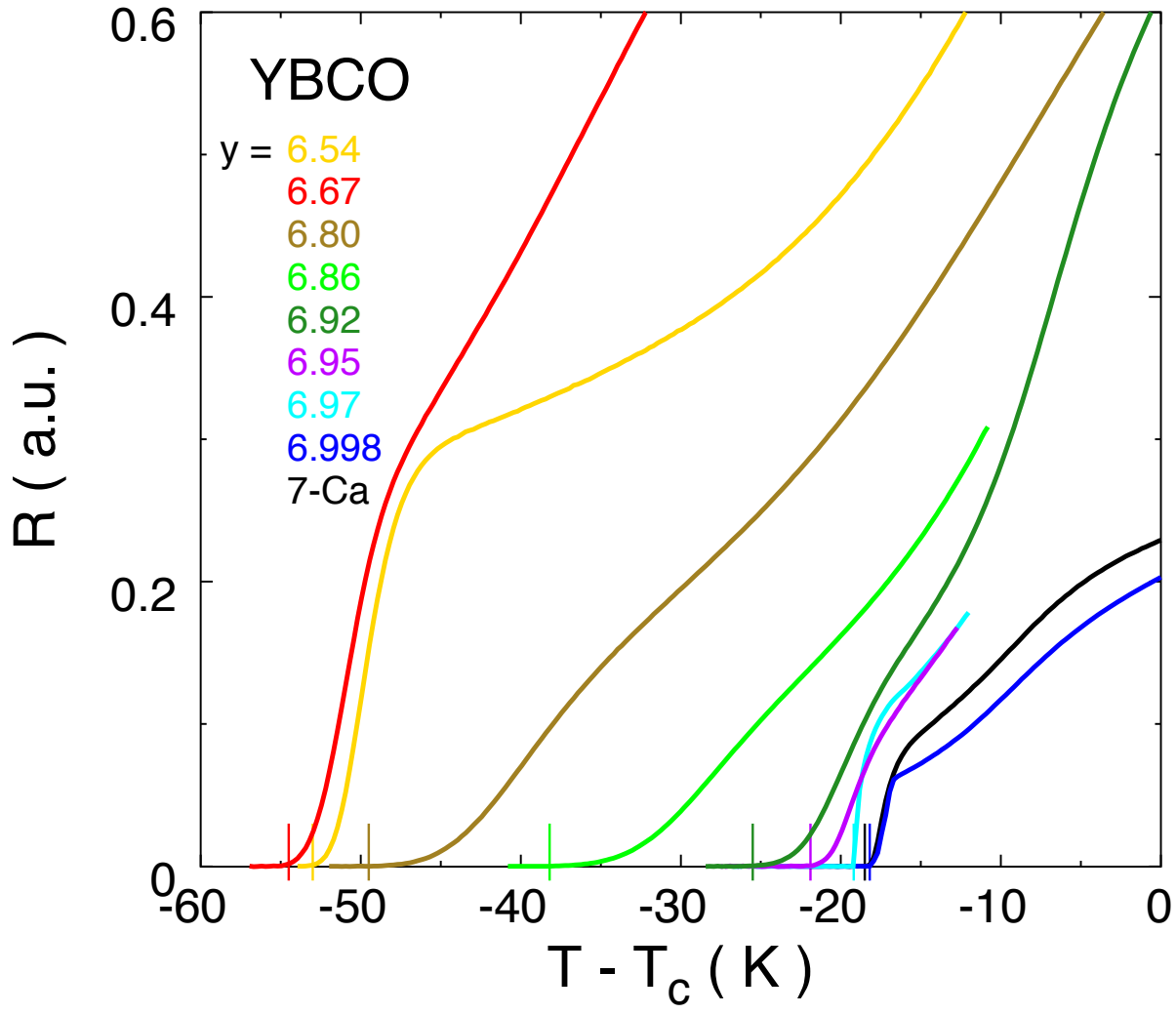


FIG. S6: Resistivity of YBCO at various dopings for $H = 15$ T. Temperature dependence of the electrical resistance $R(T)$ of 9 YBCO samples, with oxygen content y as indicated, measured in the presence of a magnetic field $H = 15$ T applied along the c axis of the orthorhombic crystal structure. The data are plotted as a function of $T/\ T_c$, where $T_c = T_c(0)$ is the zero-field superconducting transition temperature, defined as the point where R goes to zero for $H = 0$. The shift in T_c caused by the field, $\Delta T_c = T_c(15\ \mathrm{T}) - T_c(0)$, is marked by a short vertical line. It is used to obtain the sensitivity to field, defined as $-dT_c/dH = \Delta T_c/\ 15$ T. All values of $T_c(0)$, $T_c(15\ \mathrm{T})$, and $\Delta T_c/\ 15$ T are listed in Table S1.

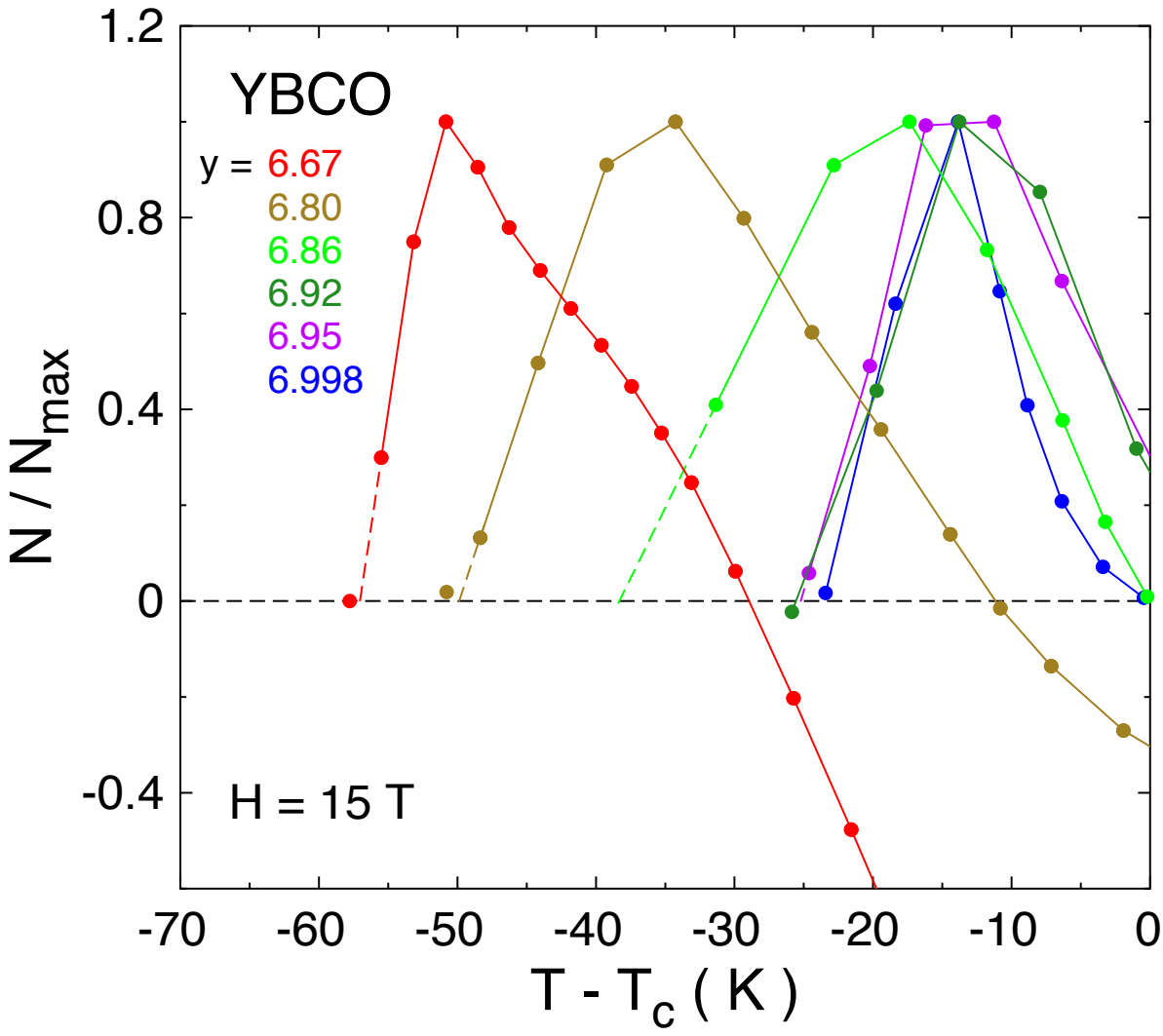


FIG. S7: Nernst signal of YBCO at various dopings for $H = 15$ T. Same as in Fig. S6, but for Nernst data instead of resistance data, measured on 6 of the samples in Fig. S6, with oxygen content y as indicated. Solid lines interconnect the data points obtained from field sweeps. Dashed lines are linear extrapolations to $N = 0$. $T_c(15\ \mathrm{T})$ is defined as the point where N goes to zero, whose values are listed in Table S1. Details on Nernst measurements can be found in ref. 20.

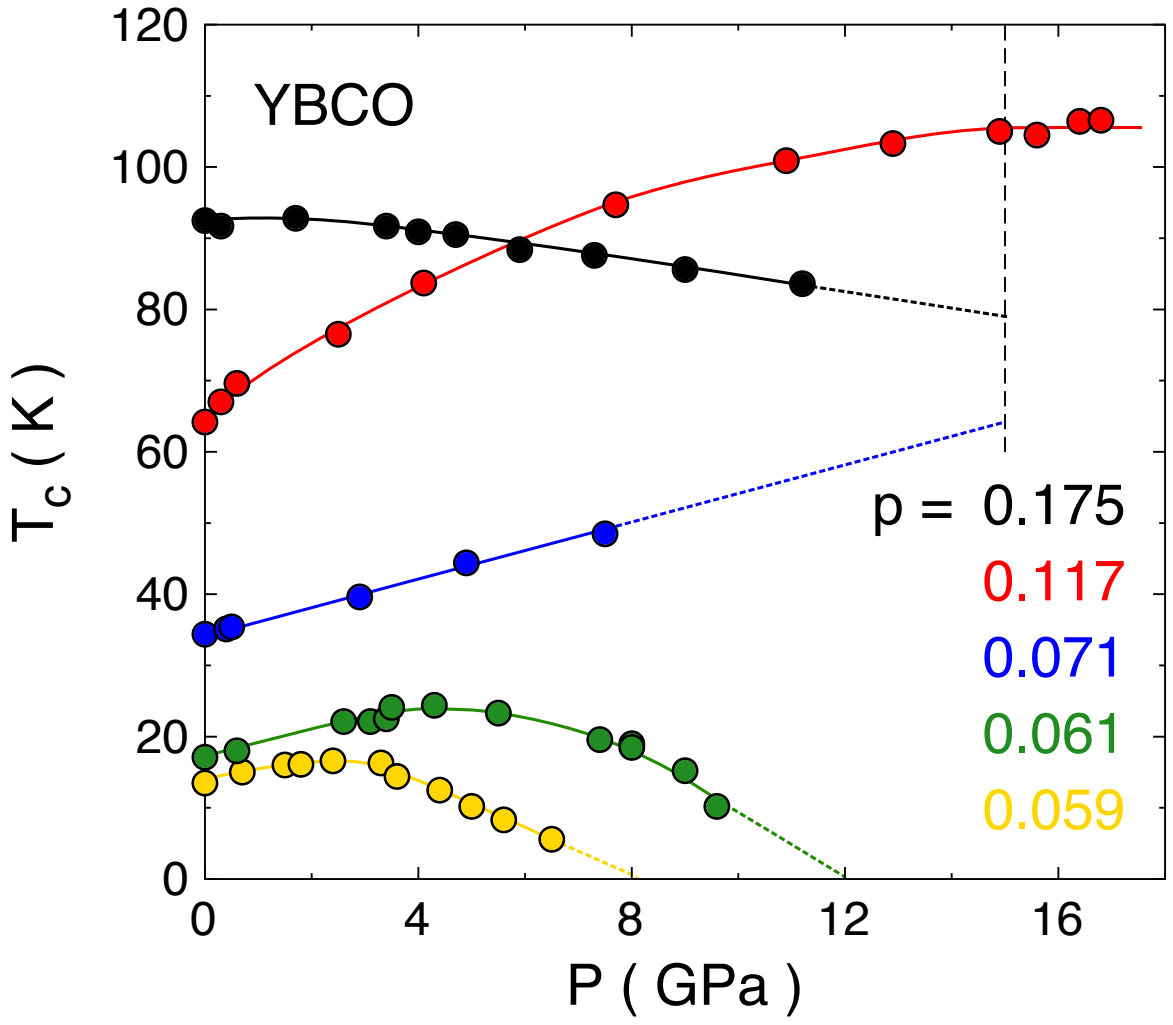


FIG. S8: Superconducting transition temperature T_c vs hydrostatic pressure P in YBCO for five dopings as indicated, reproduced from ref. 25. Note that to avoid relaxation effects due to oxygen ordering, the pressure was applied at low temperature (liquid He). Full lines are a guide to the eye. We extract the value of T_c at $P = 15$ GPa (vertical dashed line) by smoothly extrapolating the data (dotted lines). The values of T_cat $P = 15$ GPa thus obtained are plotted vs p in Fig. 4. The zero-pressure values of T_c are (from bottom to top): $T_c(0) = 14.2$ (yellow), 17.5 (green), 34.1 (blue), 63.7 (red) and 92.3 K (black) [25].

Doping effect of pressure in YBCO

There are two mechanisms by which pressure increases doping in YBCO. The first has to do with the re-arrangement of oxygen atoms in the CuO chains. Pressure improves the degree of oxygen order. With oxygen ordering comes an enhanced charge transfer between CuO chains and CuO_2 planes, and hence an increased doping of holes into the planes. This has been studied in detail (e.g. [25]), and there are two approaches to eliminate this ordering process: 1) apply pressure at a temperature of 200 K or lower; 2) use samples that already have a high degree of oxygen order.

In Table S2, we collect data on the suppression of T_c with pressure P, specifically the rate dT_c/dP, only for those studies that have used one or the other of these approaches to ensure that no oxygen relaxation effects take place. For dopings higher than $p = 0.15$, in the range where no superstructure is favoured, these precautions are not necessary. To the long list of published data, we add three data points we have taken ourselves on oxygen-ordered samples (Table S2):

$y = 6.50$, $T_c(0) = 54.5$ K, $p = 0.090$ (ortho-II order);

$y = 6.54$, $T_c(0) = 60.2$ K, $p = 0.107$ (ortho-II order);

$y = 6.67$, $T_c(0) = 65.3$ K, $p = 0.119$ (ortho-VIII order).

They fit very well with the other data (Fig. S5).

The second mechanism by which pressure increases doping is one that cannot be avoided. By bringing the chains closer to the planes, charge transfer is improved and hole doping is increased. The variation of T_c, with pressure therefore includes two terms [27, 28]:

$$\frac{\partial T_c}{\partial P} = \frac{\partial p}{\partial P}\left(\frac{\partial T_c}{\partial p}\right)_P + \left(\frac{\partial T_c}{\partial P}\right)_p . \tag{S1}$$

The term on the left of the equation is the raw "sensitivity to pressure", as measured in the experiment. The first term on the right represents the doping effect of pressure and the second term is the direct (intrinsic) dependence of T_c on P, of interest here. Fortunately, the first term is small. In Fig. S5, we plot that raw $\partial T_c/\partial P$ vs doping p (open circles) (Table S2). We immediately see a sharp peak at $p = 0.12$. To investigate the effect of pressure-induced doping on these data, we plot a corrected set of data, obtained by subtracting the product of $\partial p/\partial P$ and $(\partial T_c/\partial p)_P$. Assuming that $\partial p/\partial P$ varies linearly with p, we fix the prefactor by requiring that $(\partial T_c/\partial P)_p = 0$ for $p \geq 0.16$, in the overdoped region. This is based on our assumption that the small negative values of $\partial T_c/\partial P$ measured at $p > 0.16$ are purely due to the doping effect, since $(\partial T_c/\partial p)_P < 0$ on the downward sloping side of the T_c vs p curve. This yields $\partial p/\partial P = 0.01\,p$ hole / GPa. As for $(\partial T_c/\partial p)_P$, it is simply the derivative of the T_c vs p curve (black curve in Fig. 1), plotted as the red line in Fig. S5. The corrected data are shown as full circles. We see that the correction is small everywhere.

The bottom line is that whether we correct or not, the curve is strongly peaked at $p = 0.12$, and this peak starts below $p = 0.16$, exactly as the CDW dome (Fig. 1). Moreover, the sensitivity to pressure, whether raw or corrected, tracks the sensitivity to field at all p (Fig. 3).

In Fig. S8, the value of T_c measured in YBCO by Sadewasser *et al.* [25] at 5 different dopings is plotted vs pressure. We extrapolate these curves to $P = 15$ GPa, and hence obtain T_c at $P = 15$ GPa, plotted in Fig. 4. In that figure,

the doping values are obtained using the same formula as above, namely $p(P) = p(0) + 0.01\,P$. In Fig. S8, the data at $p(0) = 0.177$ (red) need not be extrapolated since they go up to 17 GPa. The fact that T_c for that sample becomes flat above 15 GPa implies that it has reached its maximal value, $T_c = 105$ K. This shows that the peak in the dome of T_c vs p at 15 GPa must be at $p = 0.13$ or lower. For the four other samples, extrapolations are needed to get T_c at 15 GPa. For the highest doping (black; $p(0) = 0.175$), the linear extrapolation is reasonable and the uncertainty is small, so that $T_c(15\text{ GPa}) = 80 \pm 5$ K. For the lowest two dopings, it is clear that $T_c(15\text{ GPa}) = 0$ regardless of how one extrapolates to 15 GPa. The only significant uncertainty is on the sample with $p(0) = 0.071$ (blue), whose data stop at 8 GPa. The dependence of T_c between 8 GPa and 15 GPa could be quite different from the linear extrapolation shown in Fig. S8. To reflect that uncertainty, we assign a large error bar to that point, namely $T_c(15\text{ GPa}) = 63 \pm 20$ K. Note that this large uncertainty has little impact on the superconducting dome displayed in Fig. 4. In particular, the position of the peak in the dome of T_c vs p at 15 GPa must necessarily be in the interval $0.08 < p < 0.13$, most likely close to 0.13.